

## A Model of Zymogen Factor XII: Insights into Protease Activation

Tracking no: ADV-2025-015842R1

Aleksandr Shamanaev (Vanderbilt University Medical Center, United States) Yujie Ma (University of Nottingham, United Kingdom) Michal Ponczek (University of Lodz, Poland) Mao-fu Sun (Vanderbilt University Medical Center, United States) Qiufang Cheng (Vanderbilt University Medical Center, United States) S. Dickeson (Vanderbilt University Medical Center, United States) Owen McCarty (Oregon Health & Science University, United States) Jonas Emsley (University of Nottingham, United Kingdom) Bassem Mohammed (St. Louis University School of Medicine, United States) David Gailani (Vanderbilt University Medical Center, United States)

### Abstract:

In plasma, the zymogens factor XII (FXII) and prekallikrein reciprocally convert each other to the proteases FXIIa and plasma kallikrein (PKa). PKa cleaves high-molecular-weight kininogen (HK) to release bradykinin, which contributes to regulation of blood vessel tone and permeability. Plasma FXII is normally in a "closed" conformation that limits activation by PKa. When FXII binds to a surface during contact activation it assumes an "open" conformation that increases the rate of activation by PKa. Mutations in FXII that disrupt the closed conformation have been identified in patients with conditions associated with excessive bradykinin formation. Using FXII structures predicted by AlphaFold, we generated models for the closed form of human FXII that we tested with site-directed mutagenesis. The best model predicts multiple interactions between the fibronectin type 2, kringle and catalytic domains involving highly conserved amino acids that restrict access to the FXII activation cleavage sites. Based on the model, we expressed FXII with single amino acid substitutions and studied their effects on FXII activation by PKa. Replacements for Arg36 in the fibronectin type 2 domain; Glu225, Asp253 or Trp268 in the kringle domain, or Lys346 near the activation cleavage site were activated >10-fold faster by PKa than wild type FXII. Adding these proteins to plasma resulted in rapid HK cleavage due to markedly enhanced reciprocal activation with PK. The results support a model that explains the behavior of FXII in solution. Conformational changes involving the identified amino acids likely occur when FXII binds to a surface to facilitate activation.

**Conflict of interest:** COI declared - see note

**COI notes:** D.G. receives consultants fees from pharmaceutical companies with an interest in inhibition of contact activation and the kallikrein-kinin system for therapeutic purposes.

**Preprint server:** No;

**Author contributions and disclosures:** A.S. conceived the project, expressed and purified recombinant proteins, designed and performed assays characterizing activation of FXII, PK and FXI, and contributed to writing the manuscript. Y.M. contributed to modeling FXII. M.B.P. contributed to assessment of FXII and Pro-HGFA sequences across vertebrate species. M-F.S. Developed the binding assay for assessing PK interactions with FXII and FXIIa. Q.C. conducted assays in mice. S.K.D. contributed to designing expression systems for FXII. O.J.T.M contributed to design of the project and writing of the manuscript. JE contributed to modeling work and writing the manuscript. B.M.M. conducted structural studies and contributed to writing the manuscript. D.G. oversaw the project and writing of the manuscript.

**Non-author contributions and disclosures:** No;

**Agreement to Share Publication-Related Data and Data Sharing Statement:** For readers interested in original data, sequences of cDNA constructs, or obtaining cDNA constructs used in this study, please contact David Gailani, MD at dave.gailani@vumc.org.

Clinical trial registration information (if any):

## A Model of Zymogen Factor XII: Insights into Protease Activation

Aleksandr Shamanaev<sup>1</sup>, Yujie Ma<sup>2</sup>, Michal B. Ponczek<sup>3</sup>, Mao-fu Sun<sup>1</sup>, Quifang Cheng<sup>1</sup>,  
S. Kent Dickeson<sup>1</sup>, Owen J.T. McCarty<sup>4</sup>, Jonas Emsley<sup>2</sup>, Bassem M. Mohammed<sup>5</sup>, David Gailani<sup>1</sup>.

<sup>1</sup>Department of Pathology, Microbiology and Immunology, Vanderbilt University Medical Center, Nashville, TN, USA; <sup>2</sup>Biodiscovery Institute, School of Pharmacy, University of Nottingham, Nottingham, UK; <sup>3</sup>University of Lodz, Faculty of Biology and Environmental Protection, Department of General Biochemistry, Lodz, Poland; <sup>4</sup>Department of Biomedical Engineering, School of Medicine, Oregon Health & Science University, Portland, OR, USA. <sup>5</sup>Edward A. Doisy Research Center, Department of Biochemistry and Molecular Biology, St. Louis University School of Medicine, St. Louis, MO, USA

Running title: *Factor XII Structure*

To whom correspondence should be addressed:

Aleksandr Shamanaev, Ph.D.  
Vanderbilt University Medical Center  
Room 4914 The Vanderbilt Clinic  
1301 Medical Center Drive  
Nashville, TN, USA,  
Tel. 615-936-1798.  
E-mail: [aleksandr.shamanaev@vumc.org](mailto:aleksandr.shamanaev@vumc.org)

### Agreement to Share Publication-Related Data and Data Sharing Statement:

For readers interested in original data, sequences of cDNA constructs, or obtaining cDNA constructs used in this study, please contact David Gailani, MD at [dave.gailani@vumc.org](mailto:dave.gailani@vumc.org).

**Abstract word count: 249**

**Text Word Count: 4298**

## **ABSTRACT**

In plasma, the zymogens factor XII (FXII) and prekallikrein reciprocally convert each other to the proteases FXIIa and plasma kallikrein (PKa). PKa cleaves high-molecular-weight kininogen (HK) to release bradykinin, which contributes to regulation of blood vessel tone and permeability. Plasma FXII is normally in a “closed” conformation that limits activation by PKa. When FXII binds to a surface during contact activation it assumes an “open” conformation that increases the rate of activation by PKa. Mutations in FXII that disrupt the closed conformation have been identified in patients with conditions associated with excessive bradykinin formation. Using FXII structures from the AlphaFold data base, we generated models for the closed form of human FXII that we tested with site-directed mutagenesis. The models predict multiple interactions between the fibronectin type 2, kringle and catalytic domains involving highly conserved amino acids that restrict access to the FXII activation cleavage sites. Based on the model, we expressed FXII with single amino acid substitutions and studied their effects on FXII activation by PKa. Replacements for Arg<sup>36</sup> in the fibronectin type 2 domain; Glu<sup>225</sup>, Asp<sup>253</sup> or Trp<sup>268</sup> in the kringle domain, or Lys<sup>346</sup> near the activation cleavage site were activated >10-fold faster by PKa than wild type FXII. Adding these proteins to plasma resulted in rapid HK cleavage due to markedly enhanced reciprocal activation with PK. The results support a model that explains the behavior of FXII in solution. Conformational changes involving the identified amino acids likely occur when FXII binds to a surface to facilitate activation.

## **KEY POINTS**

- When not bound to a surface, FXII adopts a “closed” conformation that is resistant to activation by plasma kallikrein.
- Intramolecular interactions between the fibronectin type 2, kringle and catalytic domains maintain the closed conformation.

## INTRODUCTION

Factor XII (FXII) is the zymogen of the plasma serine protease factor XIIa (FXIIa).<sup>1-3</sup> As part of the kallikrein-kinin system (KKS), FXIIa proteolytically converts prekallikrein (PK) to the protease plasma kallikrein (PKa).<sup>1-5</sup> PKa in turn converts FXII to FXIIa and cleaves high-molecular-weight kininogen (HK) to release bradykinin.<sup>1-5</sup> At least two mechanisms regulate the reciprocal activation process. The serpin C1-inhibitor (C1-INH) is the main plasma regulator of FXIIa and PKa.<sup>6-9</sup> In the common form of the disorder hereditary angioedema (HAE), excessive bradykinin production due to C1-INH deficiency causes episodic soft tissue swelling that can be life-threatening.<sup>7-9</sup> FXIIa and PKa inhibitors reduce angioedema in C1-INH-deficient patients, consistent with important roles for both proteases in HAE.<sup>10,11</sup> A second regulatory mechanism is intrinsic to FXII. The non-catalytic “heavy chain” of FXII restricts FXII activation by PKa, limiting the rate of FXII-PK reciprocal activation.<sup>1,3,12,13</sup> In some HAE patients, this inhibitory role is lost due to a mutation that allows the heavy chain to be separated from the rest of FXII.<sup>14-16</sup> This results in enhanced reciprocal activation that overrides the normal regulatory function of C1-INH. Reciprocal FXII-PK activation also increases when FXII and PK bind to surfaces during a process called contact activation. Here, surface-binding induces changes in FXII that negate the inhibitory effect of the heavy chain.<sup>4,5,12,17</sup>

Recent work suggests that interactions involving the fibronectin type 2 (FN2) and kringle (KNG) domains on the heavy chain maintain FXII in a functionally “closed” form in solution that is relatively resistant to activation by PKa.<sup>1,3,12,18</sup> Removal of the FXII FN2 domain,<sup>18</sup> or replacement of the FN2 or KNG domain with the corresponding domain from the homologous protein hepatocyte growth factor activator<sup>12</sup> changes FXII to a functionally “open” form that is activated by PKa at least 10-fold more rapidly than wild type FXII. The structural basis for heavy chain inhibition of FXII activation is not known as full-length structures for FXII or FXIIa are not available. Using the program AlphaFold (AF),<sup>19</sup> we studied models of human and mouse FXII that showed interactions between the FN2, KNG and catalytic domains that

restrict access to the FXII activation cleavage sites. Guided by the models, we used site-directed mutagenesis to verify the importance of specific amino acids in maintaining the FXII closed form.

## MATERIALS AND METHODS

**Reagents.** Listed in **Suppl.Fig. 1**.

**Antibodies.** Listed in **Suppl.Fig. 2**.

**Structure modeling.** A detailed description of the strategy used to prepare the human FXII model in this study is presented in **Suppl.Figs. 3A-3D**. Molecular graphics and interdomain interaction analyses of FXII structures from the AF database as well as predicted by AF version 2.3 and 3.0<sup>19-22</sup> were performed with ChimeraX software (Resource for Biocomputing, Visualization, and Informatics, University of California, San Francisco).<sup>23</sup> Based on template modelling scores, predicted alignment error values, and comparison with models for FXII from other species, we chose a structure for human FXII in complex with corn trypsin inhibitor (CTI) for further analysis. Key interdomain interactions in the final model are listed in **Table 1A**. Comparisons of FXII protein sequences from vertebrate species in the UniProt and NCBI databases were performed as described (**Suppl.Fig. 4**).<sup>24,25</sup>

**Recombinant proteins.** Preparation of recombinant wild type and variant human and mouse FXIIs is described in **Suppl.Fig. 5**. Amino acid substitutions introduced into human FXII are listed in **Table 1B**.

**Chromogenic assays.** Experiments were conducted in PEG-20000 coated polypropylene tubes. FXII (100nM) was incubated with 12.5nM PKa or 2.5nM FXIa in HEPES Buffer (20mM N-2-hydroxyethylpiperazine-N9-2-ethane-sulfonic acid pH7.4, 100mM NaCl, 0.1% PEG-8000) at 37°C. Aliquots (20µL) were removed at various times and reactions were stopped with Polybrene (0.1mg/mL) and soybean trypsin inhibitor (500nM). S-2302 (500µM final concentration) was added and rates of substrate cleavage ( $\Delta$ OD405nm/min) were determined on a spectrophotometer. Protease generated was derived from standard curves made with pure FXIIa. Results are averages of three separate experiments.

**FXII cleavage assessed with SDS-PAGE.** FXII (1 $\mu$ M) was incubated with 125nM PKa in HEPES Buffer. At various times, aliquots were removed into reducing sample buffer, size-fractionated on NuPAGE 4-12% Bis-Tris gradient gels (Invitrogen), and stained with Coomassie blue. Densitometry analysis of FXII zymogen band disappearance was performed with GelAnalyzer 19.1 software (I. Lazar Jr. and I. Lazar Sr., [www.gelanalyzer.com](http://www.gelanalyzer.com); last accessed 10/10/2023).

**Western blots of human plasma.** Reactions were run in PEG 20000-coated polypropylene tubes. FXII-deficient plasma (40 $\mu$ L) was mixed with phosphate-buffered saline (PBS, 80 $\mu$ L) containing FXII (final concentration 130nM) and incubated in the absence or presence of kaolin (40 $\mu$ g) at 37°C. Aliquots were removed at various times into nonreducing SDS-sample buffer, size fractionated on 7.5% polyacrylamide-SDS gels, and transferred to nitrocellulose. FXII, PK and XI activation were analyzed by western blot using horseradish peroxidase conjugated (HRP-conjugated) polyclonal IgGs and chemiluminescence as described.<sup>26</sup> For assessing HK cleavage, a polyclonal primary IgG and fluorescent secondary IgG were used. Densitometry was performed with GelAnalyzer version 19.1.

**FXII binding assay.** 96-well microtiter plates were coated overnight at 4°C with 100 $\mu$ L 50mM carbonate buffer pH9.6 containing 20 $\mu$ g/mL anti-PK IgG 5C8,<sup>27</sup> blocked with PBS containing 2% bovine serum albumin (BSA) at room temperature (RT) for 60 min, then washed 3 $\times$  with PBS/0.1% Tween-20. Wells were filled with 100 $\mu$ L diluent buffer (90mM HEPES pH7.2, 100mM NaCl, 1%BSA, 0.1%Tween-20) containing PK (5 $\mu$ g/mL) for 90 min, followed by 100 $\mu$ L diluent buffer containing FXII or FXIIa for 90 min. HRP-conjugated anti-hemagglutinin IgG (1:5000) in 100 $\mu$ L diluent buffer was added for 90 min, then 100 $\mu$ L Substrate Solution (5mg *o*-phenylenediamine in 12ml citrate-phosphate pH5.0 with 12 $\mu$ l 30% H<sub>2</sub>O<sub>2</sub>) was added. Reactions were stopped after 15 min with 50 $\mu$ l 2.5M H<sub>2</sub>SO<sub>4</sub>, and OD490nm was measured. Values for 30 $\mu$ g/ml recombinant wild type FXII (FXII-WT) represent 100% binding.

**FXII pull-down assay.** Protein G Agarose-beads (25 $\mu$ l) were mixed with IgG 5C8 (30 $\mu$ g), incubated for 2 hrs at RT, then washed 3 $\times$  with Tris-Buffered Saline (TBS). In experiment 1, 5C8-beads were mixed with 10 $\mu$ g plasma FXII or FXIIa, alone or with PK. In experiment 2, PK lacking an active site serine (PK-Ala559)<sup>28</sup> was mixed with plasma FXII, or recombinant FXII. Reactions were incubated overnight (~14

hrs) at 4°C with rotation in the presence of 5µM FPRCK. Beads were washed 3× with TBS and eluted with nonreducing SDS-sample buffer. Samples were size fractionated on 10% polyacrylamide-SDS gels and either stained with Coomassie blue (experiment 1) or transferred to nitrocellulose and probed with anti-FXII HRP-conjugated IgG (experiment 2). Each reaction was performed in duplicate.

**Activated Partial Thromboplastin Time Assay.** Described in **Suppl.Fig. 6**.

**Single Molecule Förster Resonance Energy Transfer (smFRET).** Described in **Suppl.Fig. 7**.

**HK cleavage in mice.** Procedures with mice were approved by the Vanderbilt University Animal Care and Use Committee. FXII (0.15mg/kg) in 50µL PBS was infused into FXII-deficient C57Bl/6 mice through a tail vein. Plasma was prepared from blood collected from tail veins into a 1/10<sup>th</sup> volume of 3.2% sodium citrate and analyzed by non-reducing western blots with rabbit anti-mouse HK IgG.<sup>16</sup>

## RESULTS

**A model for human FXII.** **Fig. 1A** shows a schematic diagram of the human FXII polypeptide. A short sequence at the N-terminus is followed by fibronectin type 2 (FN2), first epidermal growth factor (EGF1), fibronectin type 1 (FN1), second epidermal growth factor (EGF2) and kringle (KNG) domains, a proline-rich region (PRR), an activation loop (Cys340 to Arg353) and a catalytic domain (CD).<sup>1,3</sup> During conversion to α-FXIIa, FXII is cleaved by PKa after Arg353, converting the catalytic domain into a fully active conformation.<sup>1-5</sup> A second cleavage of unknown significance occurs after Arg343.<sup>3,29</sup>

The model for human FXII in the AF database (AF P00748, **Suppl.Fig. 3A**) was described by Frunt et al.<sup>30</sup> It differs from AF FXII models for most terrestrial vertebrates in several respects. A comparison of the P00748 FXII model with the mouse model (Q80YC5, **Suppl.Fig. 3B**) shows the CD of P00748 rotated with respect to the rest of the molecule. Because of this rotation, a highly conserved bond between the side chain of Lys346 in the activation loop and an Asp251-Asn-Asp253 motif on the KNG domain is missing. Indeed, in P00748 the KNG domain and activation loop are relatively distant and are not predicted to interact. We performed analyses of P00748 using AF-Multimer software and identified conditions that altered the P00748 structure so that it forms the Lys346 interaction with Asp251-Asn-

Asp253 (**Suppl.Fig. 3C-3D**). The highest confidence score was for a model of human FXII in complex with the inhibitor CTI (**Suppl.Fig. 3E**). A subsequent FXII structure obtained with AF version 3.0 predicted the Lys346-KNG interaction (**Suppl.Fig. 3F**), as well as many other intramolecular interactions observed in models in **Suppl.Figs. 3B-3D**, without the need for CTI. Based on our analysis we chose the structure for human FXII in complex with CTI (**Suppl.Figs. 3C**) as a guide for mutagenesis studies and concluded that the outlier status of the original P00748 structure reflected errors in the database model.

In the model in **Fig. 1B**, domains in the non-catalytic heavy chain region form a ring-like structure, with multiple hydrogen bonds forming between the FN2 and KNG domains, KNG and the activation loop, and FN2 and the CD. AF did not assign a structure to the PRR, displaying it as a disordered and highly extended linker (**Suppl.Fig. 3C**). The PRR is removed from images in **Fig. 1B** for clarity. The FXII activation cleavage sites at Arg353 and Arg343 are on opposite faces of the molecule (dark blue in **Fig. 1B**). The activation peptide between these residues is buried between the KNG and CD. Furthermore, the Arg353-Val354 and Arg343-Leu344 bonds that are cleaved during FXII activation are also buried in the structure, perhaps explaining why FXII in solution is activated relatively slowly by PKa.

The model predicts 22 electrostatic interactions between residues on FN2, KNG, the activation loop and CD (**Fig. 1C**, listed in **Table 1A**) that appear to be important for the structure of the heavy chain and its relationship to the activation peptide and CD. Two clusters of interactions involving Lys346 in the activation loop and Arg36 in the FN2 domain appear to be central to the structure. As discussed, Lys346 interacts with the Asp251-Asn-Asp253 consensus binding site in the KNG domain. It also forms cation- $\pi$  bonds with Trp257 and Trp268 on KNG. Arg36 forms electrostatic bonds with Glu225 in the KNG domain and Glu502 in the CD, and hydrophobic contacts with Leu266 (KNG) and Val359 (CD). The residues shown in **Fig. 1C** are conserved across species (**Suppl.Fig. 4**) and form bonds with other conserved residues (**Table 1A**).

**Closed and Open Forms of FXII.** As discussed, FXII-WT is activated relatively slowly by PKa when not bound to a surface.<sup>12,28,31</sup> For purposes of this study, the rate for this reaction represents the “closed” form of FXII (**Figs. 2A and 2B**). We reported that  $\Delta$ FXII, which lacks a heavy chain, is activated by PKa  $\sim$ 10-

40 fold faster than FXII-WT in the absence of a surface (**Fig. 2A** and **2B**).<sup>12,16</sup> For this study, the activation rate for  $\Delta$ FXII represents a functionally “open” form of FXII. These terms will be applied to recombinant FXII variants in the following sections solely to indicate their susceptibility to activation. While introduced mutations likely cause conformational changes that render FXII more susceptible to activation by PKa, the terms “closed” and “open” are not meant to imply specific structural changes.

**Recombinant FXII.** To establish the importance of the amino acids in **Table 1A** for maintaining FXII in a closed form, FXII cDNAs encoding alanine replacements of single amino acids were prepared (**Table 1B**, **Suppl.Fig. 5**). We studied twelve conserved residues (Arg36, Asp61, Glu225, Asp253, Leu266, Trp268, Arg343, Lys346, Val359, Gln501, Glu502, and Glu551) and six non-conserved residues (Lys45, Asp264, Arg265, Arg345, Arg362, and Glu411) predicted to be involved in intramolecular interactions. Three residues not predicted to form interdomain interactions (Lys41, Lys47, and Asn230) were selected for controls. As the Asp251/Asp253 and Trp257/Trp268 pairs are predicted to interact with a single amino acid (Lys346), we only analyzed replacements for Asp253 and Trp268.

FXII-Ala253 was unstable in culture, so we replaced it with FXII-Lys253.<sup>12</sup> FXII-Ala61 was not secreted, and FXII-Ala268 and FXII-Ala502 were heavily proteolyzed (**Suppl.Fig. 5B**). FXII-Ala268 and FXII-Ala502 were modified by replacing the active site serine (Ser544) with alanine (FXII-Ala268,544 and FXII-Ala502,544). This stabilized both proteins (**Suppl.Figs. 5B**), indicating proteolysis was at least partly autocatalytic. All other variants were expressed as stable zymogens (**Suppl.Figs. 5A**) that had activity in an aPTT assay comparable to FXII-WT (**Suppl.Fig. 6**). This indicates the substitutions did not disrupt surface-mediated FXII activation or  $\alpha$ -FXIIa activation of PK or FXI.

**FXII Activation.** Most FXII variants were activated by PKa similarly or only slightly faster than FXII-WT (**Figs. 2A** and **2B**). Four variants, FXII-Ala36, FXII-Ala225, FXII-Lys253, and FXII-Ala346 were activated comparably to  $\Delta$ FXII (**Figs. 2A** and **2B**) consistent with a functionally open conformation. FXII-Ala266, which is predicted to form a hydrophobic bond with Ala36, was activated at an intermediate rate between those of FXII-WT and  $\Delta$ FXII (**Figs. 2A**). FXIa is a homolog of PKa that also activates

FXII.<sup>3</sup> FXIa activated  $\Delta$ FXII, FXII-Ala36, FXII-Ala225, FXII-Lys253 and FXII-Ala346 at comparable rates and, as with PKa, activated FXII-Ala266 at an intermediate rate (**Fig. 2C**).

Proteolytic cleavage of FXII after Arg353 and Arg343 converts the 80 kDa FXII polypeptide to the 50-kDa heavy chain and 30-kDa light chain (catalytic domain) of  $\alpha$ -FXIIa (**Fig. 2D**). On reducing SDS-PAGE, loss of the 80 kDa band is more rapid with FXII-Ala346 than with FXII-WT (**Figure 2D**). To verify that the amidolytic activity in **Figs. 2A-2C** reflects conversion of FXII to FXIIa, and not changes in FXIIa catalytic efficiency between variants, we compared cleavage of FXII variants to FXII-WT by reducing SDS-PAGE, and densitometry (**Fig. 2E**). Variants displaying the highest activities in the amidolytic assay had more rapid disappearance of the 80 kDa band, consistent with increased conversion to FXIIa. Activation of FXII-Ala268,544 and FXII-Ala502,544 could not be analyzed by activity-based assays because the proteins lack active site serine residues. However, their cleavage can be assessed by the SDS-PAGE approach. FXII with alanine replacing Ser544 (FXII-Ala544), FXII-Ala268,544 and FXII-Ala502,544 were incubated with PKa. FXII-Ala268,544 is activated more rapidly than FXII-Ala544 (**Fig. 2F**) and comparably to FXII-Ala346 (**Fig. 2D**), while FXII-Ala502,Ala544 is activated moderately faster than FXII-Ala544 (**Fig. 2F**).

Mixing FXII and PK in solution results in reciprocal conversion to FXIIa and PKa by a process initiated by activity intrinsic to the FXII zymogen (**Suppl.Fig. 7A**).<sup>3,12,13,16,29</sup> Reciprocal activation is more rapid in reactions with FXII-Ala36, FXII-Ala225, FXII-Lys253 and FXII-Ala346 compared with FXII-WT (**Suppl.Fig. 7B**), and comparable to reactions with  $\Delta$ FXII (**Suppl.Fig. 7A**).<sup>3,12,13,16,29</sup> The FXII variants do not spontaneously activate in the absence of PK and are not activated faster by FXIIa (**Suppl.Fig. 8**), suggesting the open conformation primarily facilitates activation by PKa. Taken as a whole, the data support the conclusion that non-covalent interactions involving Arg36 on the FN2 domain; Glu225, Asp251/Asp253, Trp268 and Val266 on the KNG domain, and Lys346 on the activation peptide are involved in maintaining the FXII closed conformation. The importance of the interactions centered on Arg36 and Lys346 are supported by mutagenesis studies with mouse FXII (m $\Delta$ FXII, **Suppl.Fig. 9**).

**FXII KNG Domain.** Previously, Ravon *et al* showed that an IgG (F1) to the FXII KNG domain induced slow FXII autoactivation.<sup>32</sup> The anti FXII IgG 5A12 recognizes the FXII heavy chain,<sup>33</sup> and like F1, induces autoactivation of FXII-WT (**Figs. 3A** and **3B**) as well as of FXII-Ala36 and FXII-Ala346 (**Fig. 3B**). It did not induce autoactivation of  $\Delta$ FXII, which lacks a heavy chain (**Fig. 3B**). Interestingly, 5A12 did not induce autoactivation of FXII-Lys253 (**Fig. 3B**). On Western blots, 5A12 recognizes FXII-WT,  $\alpha$ -FXIIa, and FXII-Ala346, but not FXII-Lys253. This suggests that Asp253 is at or near the 5A12 recognition site (**Fig. 3C**) and implies that 5A12 may disrupt the KNG interaction with Lys346. Consistent with this, 5A12 increases the rate of FXII activation by PKa (**Fig. 3D**). As shown in (**Suppl.Fig. 8**), FXII-Ala346 are not susceptible to activation by FXIIa in solution. This suggests that the ability of 5A12 to induce autoactivation does not solely reflect its effect on FXII conformation. The bivalent antibody may serve as a contact surface by bringing two FXII molecules into proximity to each other.

**FXII smFRET.** Previously, we showed that the lysine analog  $\epsilon$ ACA accelerates FXII/PK reciprocal activation, possibly by disrupting a lysine/arginine binding interaction involving the FXII KNG domain [12]. We labeled the FN2 domain and CD of FXII lacking an active site serine residue (FXII-Ser544) with the FRET pair AF555 and AF647 (**Suppl.Fig. 10**). In the absence of  $\epsilon$ ACA (**Fig. 3E, left panel**) the FRET efficiency (0.97) indicates the FRET pair are separated by  $\leq 29 \text{ \AA}$  ( $\pm 0.72 \text{ \AA}$ ) (**Suppl.Fig. 10**). This is in agreement with the model of FXII in complex with CTI (**Fig. 1B**), but not with the original AF P00748 model (**Suppl.Fig. 3A**) where the estimated distance between the fluorophores is  $\sim 40 \text{ \AA}$ .  $\epsilon$ ACA causes a large shift centered around a FRET efficiency of 0.05 (**Fig. 3E, right panel**) indicating a displacement of FN2 away from the CD ( $\geq 74 \pm 8 \text{ \AA}$ ) with a small population still displaying high FRET efficiency consistent with the original FXII form.

**FXII binding to PK.** FXII-WT binds weakly to PK immobilized by an antibody (5C8) to its catalytic domain, while  $\alpha$ -FXIIa-WT binds with greater affinity (**Figs. 4A** and **4B**). This suggests that conversion of FXII to  $\alpha$ -FXIIa exposes a PK binding site. FXII variants with purported open structures (FXII-Ala36, FXII-Ala225, FXII-Ala346) bind to PK in their zymogen forms comparably to  $\alpha$ -FXIIa, while closed

forms (FXII-Ala47, FXII-Ala264, FXII-Ala345, FXII-Ala551) bind similarly to FXII-WT (**Fig. 4B**). FXII binding to PK in solution was tested in a pull-down assay using IgG 5C8 bound to agarose beads. In the absence of PK, neither FXII nor FXIIa are removed from solution (**Fig. 4C**). A mixture of PK and FXIIa, but not PK and zymogen FXII, results in precipitation of both proteins. The interaction between recombinant FXII-WT and PK is weak (**Fig. 4D**), but variants FXII-Lys253, FXII-Ala225 and FXII-Ala346 were precipitated with PK more efficiently (**Fig. 4D**). PK lacking an active site serine (PK-Ala559) was used in the latter experiments to avoid FXII activation. These results indicate that conversion of FXII from a functionally closed form to an open form involves conformational changes that expose a binding site for PK.

***FXII Activation of the Kallikrein-Kinin System.*** In FXII-deficient plasma reconstituted with FXII-WT, inducing contact activation with kaolin leads to decreased intensity of FXII, PK and FXI bands, and formation of high-molecular-weight species representing FXIIa, PKa and FXIa in complex with plasma inhibitors (**Fig. 5A, top**).<sup>26</sup> These changes do not occur in the absence of kaolin (**Fig. 5A, bottom**). In the absence of kaolin, reconstituting FXII-deficient plasma with FXII-Ala36 (**Fig. 5B, top**) or FXII-Ala346 (**Fig. 5B, bottom**) causes changes in FXII and PK similar to those induced by kaolin in plasma with FXII-WT. This is consistent with open forms of FXII accelerating reciprocal activation with PK independently of a surface., FXIIa is a poor FXI activator in the absence of a surface,<sup>26,27</sup> explaining the apparent absence of FXI activation in experiments with FXII-Ala36 and FXII-Ala346 (**Fig. 5B, right column**).

Previously, we showed that adding  $\Delta$ FXII, but not FXII-WT, to human plasma causes rapid HK cleavage due to accelerated PK conversion to PKa (**Fig. 6A, top**).<sup>16</sup> Rapid HK cleavage also occurs if FXII-Ala36, FXII-Lys253, or FXII-Ala346 are added to plasma (**Fig. 6A, bottom**). Similarly, infusing  $\Delta$ FXII, FXII-Ala36, FXII-Lys253, or FXII-Ala346 into FXII-deficient mice leads to rapid HK cleavage, while infusing FXII-WT does not (**Fig. 6B**). These data show that open forms of FXII accelerate PK activation and HK cleavage in plasma, likely by overwhelming the capacity of C1-INH to control FXII and PK activation.<sup>16</sup>

## DISCUSSION

FXIIa contributes to bradykinin generation by activating PK, and drives contact activation-induced coagulation by activating FXI.<sup>1-5</sup> PKa, in turn, activates FXII at a relatively slow rate in solution.<sup>3,17,26,31</sup> The KKS probably continuously idles at a low-level by this process.<sup>34,35</sup> Dysregulation of this process leads to excessive bradykinin production in the genetic disorder HAE. In one form of HAE, a mutation in the FXII PRR introduces a protease cleavage site that allows separation of the heavy chain from the CD.<sup>15-17</sup> The resulting truncated FXII species ( $\Delta$ FXII) is activated 10-40 times more rapidly than full-length FXII, implying the heavy chain normally restricts the rate of FXII activation in solution. Prior work implicated two parts of the heavy chain, the FN2 and KNG domains, in this regulatory role.<sup>3,16,18</sup> The goal of the work presented here is to propose a model for human FXII that explains the effect of the heavy chain on FXII activation, and specifically the effects of the FN2 and KNG domains on this process. Crystal structures are available for the FXII CD and parts of the heavy chain,<sup>35-38</sup> but there is no structure for the whole molecule that provides information regarding the relationship of the heavy chain to the CD. To address this, we modeled human FXII using AF.<sup>19-22</sup> Previously, Frunt *et al.* described a model in the AF database for human FXII designated P00748.<sup>30</sup> A feature of this model is that the heavy chain forms a circular structure with the FN2 domain interacting with the KNG domain. This intriguing observation seemed relevant to observations with recombinant FXII chimeras indicating that FN2 and KNG are required for the heavy chain to restrict FXII activation.<sup>12,18</sup> However, P00748 lacks many of the intramolecular bonds between FN2, KNG and the catalytic domain predicted for most other vertebrate FXII structures. In particular, a bond between the Lys<sup>346</sup> side chain and a binding site for Lys/Arg acid side chains (Asp<sup>251</sup>-X-Asp<sup>253</sup>) found in nearly all FXII models, was absent from P00748. The model we selected for guiding mutagenesis was obtained by simulating binding of the inhibitor CTI with P00748. In this model, there were extensive interactions between the FN2 and KNG domains, FN2 and the CD, and the activation loop and KNG that were similar to those found in mouse FXII. Subsequent modeling with a more recent version of AF (version 3.0) agreed with the model we selected, but did not require CTI. Of note, in FXII bound to CTI the peptide bonds cleaved by PKa to convert FXII to  $\alpha$ -FXIIa are buried

between the CD and KNG domains. This feature, which provides an explanation for the slow rate of activation of FXII by PKa, is not found in the original P00748 structure.

We refer to FXII-WT as being in a “closed” form that is relatively resistant to activation, while truncated  $\Delta$ FXII and some full-length FXII variants are in an “open” form that is activated at a rate at least 10-fold higher than for FXII-WT.<sup>12,13,16,17</sup> These terms are used here ~~exclusively~~ as functional definitions that describe sensitivity to PKa, and not to imply specific conformational changes in each structure. However, we recognize that transition from the closed to an open form may involve conformational changes that expose the activation cleavage sites and a binding site for PK. Previously, we showed that the lysine analog  $\epsilon$ -ACA increases the rate of FXII activation by PKa.  $\epsilon$ -ACA has a similar effect on activation of plasminogen and prothrombin,<sup>39,40</sup> where it inhibits interactions between lysine/arginine side chains and KNG domains. In smFRET studies,  $\epsilon$ -ACA appeared to induce a major change in FXII conformation, as reflected by the change in position of the FN2 domain relative to the CD. While we were not able to determine if similar changes accompany mutations that open the FXII structure, the results raise the possibility that conversion of FXII in a closed form to an open form involves significant conformational change.

The conserved residues Lys<sup>346</sup> and Arg<sup>36</sup> are central to the model for the closed form of FXII. Lys<sup>346</sup>, located between the activation cleavage sites at Arg<sup>343</sup> and Arg<sup>353</sup>, forms a hydrogen bond with the consensus binding site for basic amino acids (Asp<sup>251</sup>-Asn-Asp<sup>253</sup>) on the KNG domain. The open structures of FXII-Lys<sup>253</sup> and FXII-Ala<sup>346</sup>, as reflected by their high rate of activation by PKa, support the conclusion that this interaction is important to the closed structure. This is supported by the effect of IgG 5A12, which binds in proximity to FXII Asp<sup>253</sup>, on FXII activation. It is possible that cleavage of Arg<sup>343</sup> and Arg<sup>353</sup> during FXII activation allows the activation peptide to retract with the KNG domain away from the CD. Our analysis also indicates that a bond between Arg<sup>36</sup> on the FN2 domain and Glu<sup>225</sup> on the KNG domain are required for the closed conformation, perhaps with a contribution from an interaction between the alkyl group of the Arg<sup>36</sup> sidechain and the Leu<sup>266</sup> sidechain. FXII binds several proteins on endothelial cell surfaces, including the globular C1q receptor (gC1qR).<sup>36,41</sup> Kaira *et al.*

reported that the isolated FN2 domain binds to gC1qR, and Arg<sup>36</sup> forms one of two points of contact between them.<sup>37</sup> Moreover, we observed accelerated FXII activation by PKa in the presence of gC1qR (Aleksandr Shamanaev, PhD, and David Gailani, MD, unpublished data). Perhaps FXII binding to gC1qR opens the structure by disrupting intramolecular interactions involving Arg<sup>36</sup>.

The results presented here support the hypothesis that FXII circulates in plasma in a form that is relatively resistant to activation by PKa, with interactions between residues on the FN2 domain (Arg<sup>36</sup>) and the KNG domain and CD, and between the activation loop (Lys<sup>346</sup>) and the KNG domain, critical to the structure. It follows that environments that disrupt these interactions will facilitate FXII activation. FXII activation is enhanced by binding to polyanions such as polyphosphate and to surfaces such as kaolin or silica.<sup>1-5</sup> Previously, we showed that polyphosphate binding to an anion-binding site on the FXII EGF1 domain increases the rate of FXII activation.<sup>31</sup> Engaging the anion-binding site may lead to disruption of the bonds involving Arg<sup>36</sup> and/or Lys<sup>346</sup> as part of the mechanism for surface-induced contact activation. The FXII model presented here is not complete. Our inability to model the FXII PRR is a limitation of this study. The length and amino acid composition of the PRR varies significantly between species, suggesting structural heterogeneity. Ultimately, full-length structures for FXII and FXIIa are needed to fully understand the structural changes that accompany FXII activation.

## **ACKNOWLEDGEMENTS**

The authors wish to acknowledge generous support from the National Heart, Lung and Blood Institute of the National Institutes of Health (R35 HL140025, R01HL144113) and the Ernest W. Goodpasture Chair in Experimental Pathology for Translational Research, Vanderbilt University Medical Center.

## **AUTHORSHIP**

A.S. conceived the project, expressed and purified recombinant proteins, designed and performed assays characterizing activation of FXII, PK and FXI, and contributed to writing the manuscript. Y.M. contributed to modeling FXII. M.B.P. contributed to assessment of FXII and Pro-HGFA sequences across vertebrate species. M-F.S. Developed the binding assay for assessing PK interactions with FXII and

FXIIa. Q.C. conducted assays in mice. S.K.D. contributed to designing expression systems for FXII. O.J.T.M contributed to design of the project and writing of the manuscript. JE contributed to modeling work and writing the manuscript. D.G. oversaw the project and writing of the manuscript. B.M.M. conducted structural studies and contributed to writing the manuscript.

### POTENTIAL CONFLICTS OF INTEREST

D.G. receives consultant fees from pharmaceutical companies with an interest in inhibition of contact activation and the kallikrein-kinin system for therapeutic purposes. All other authors have no conflicts to report.

### BIBLIOGRAPHY

1. de Maat S, Maas C. FXII: form determines function. *J Thromb Haemost.* 2016;14:1498-1506.
2. Maas C, Renné T Coagulation factor XII in thrombosis and inflammation. *Blood* 2018;131:1903–1909.
3. Shamanaev A, Litvak M, Ivanov I, Srivastava P, Sun MF, Dickeson SK, Kumar S, He TZ, Gailani D. Factor XII structure-function relationships. *Semin Thromb Hemost.* 2024;50:937-952.
4. Schmaier AH. The contact activation and kallikrein/kinin systems: pathophysiologic and physiologic activities. *J Thromb Haemost.* 2016;14:28-39.
5. Long AT, Kenne E, Jung R, Fuchs TA, Renne´ T. Contact system revisited: an interface between inflammation, coagulation, and innate immunity. *J Thromb Haemost.* 2016;14:427–437.
6. Karnaukhova E. C1-inhibitor: structure, functional diversity and therapeutic Development. *Curr Med Chem.* 2022;29:467–488.
7. De Maat S, Hofman ZLM, Maas C. Hereditary angioedema: the plasma contact system out of control. *J Thromb Haemost.* 2018;16:1674-1685.
8. Schmaier AH. The hereditary angioedema syndromes. *J Clin Invest.* 2019;129:66-68.
9. Petersen RS, Fijen LM, Levi M, Cohn DM. Hereditary Angioedema: The Clinical Picture of Excessive Contact Activation. *Semin Thromb Hemost.* 2024;50:978-988.
10. Banerji A, Riedl MA, Bernstein JA, Cicardi M, Longhurst HJ, Zuraw BL, Busse PJ, Anderson J, Magerl M, Martinez-Saguer I, Davis-Lorton M, Zanichelli A, Li HH, Craig T, Jacobs J, Johnston DT,

- Shapiro R, Yang WH, Lumry WR, Manning ME, Schwartz LB, Shennak M, Soteres D, Zaragoza-Urdaz RH, Gierer S, Smith AM, Tachdjian R, Wedner HJ, Hebert J, Rehman SM, Staubach P, Schranz J, Baptista J, Nothaft W, Maurer M; HELP Investigators. Effect of Lanadelumab Compared With Placebo on Prevention of Hereditary Angioedema Attacks: A Randomized Clinical Trial. *JAMA*. 2018;320:2108-2121.
11. Craig TJ, Reshef A, Li HH, Jacobs JS, Bernstein JA, Farkas H, Yang WH, Stroes ESG, Ohsawa I, Tachdjian R, Manning ME, Lumry WR, Saguer IM, Aygören-Pürsün E, Ritchie B, Sussman GL, Anderson J, Kawahata K, Suzuki Y, Staubach P, Treudler R, Feuersenger H, Glassman F, Jacobs I, Magerl M. Efficacy and safety of garadacimab, a factor XIIa inhibitor for hereditary angioedema prevention (VANGUARD): a global, multicentre, randomised, double-blind, placebo-controlled, phase 3 trial. *Lancet*. 2023;401:1079-1090.
  12. Shamanaev A, Ivanov I, Sun MF, Litvak M, Srivastava P, Mohammed BM, Shaban R, Maddur A, Verhamme IM, McCarty OJT, Law RHP, Gailani D. Model for surface-dependent factor XII activation: the roles of factor XII heavy chain domains. *Blood Adv*. 2022;6:3142-3154.
  13. Shamanaev A, Dickeson SK, Ivanov I, Litvak M, Sun MF, Kumar S, Cheng Q, Srivastava P, He TZ, Gailani D. Mechanisms involved in hereditary angioedema with normal C1-inhibitor activity. *Front Physiol*. 2023;14:1146834.
  14. Dewald G, Bork K. Missense mutations in the coagulation factor XII (Hageman factor) gene in hereditary angioedema with normal C1 inhibitor. *Biochem Biophys Res Commun*. 2006;343:1286-1289.
  15. de Maat S, Björkqvist J, Suffritti C, Wiesenekker CP, Nagtegaal W, Koekman A, van Dooremalen S, Pasterkamp G, de Groot PG, Cicardi M, Renné T, Maas C. Plasmin is a natural trigger for bradykinin production in patients with hereditary angioedema with factor XII mutations. *J Allergy Clin Immunol*. 2016;138:1414-1423.
  16. Ivanov I, Matafonov A, Sun MF, Mohammed BM, Cheng Q, Dickeson SK, Kundu S, Verhamme IM, Gruber A, McCrae K, Gailani D. A mechanism for hereditary angioedema with normal C1 inhibitor: an inhibitory regulatory role for the factor XII heavy chain. *Blood* 2019;133:1152–1163.

17. Shamanaev A, Litvak M, Gailani D. Recent advances in factor XII structure and function. *Curr Opin Hematol.* 2022;29:233-243.
18. Clark CC, Hofman ZLM, Sanrattana W, den Braven L, de Maat S, Maas C. The Fibronectin Type II Domain of Factor XII Ensures Zymogen Quiescence. *Thromb Haemost.* 2020;120:400-411.
19. Jumper J, Evans R, Pritzel A, Green T, Figurnov M, Ronneberger O, Tunyasuvunakool K, Bates R, Židek A, Potapenko A, Bridgland A, Meyer C, Kohl SAA, Ballard AJ, Cowie A, Romera-Paredes B, Nikolov S, Jain R, Adler J, Back T, Petersen S, Reiman D, Clancy E, Zielinski M, Steinegger M, Pacholska M, Berghammer T, Bodenstein S, Silver D, Vinyals O, Senior AW, Kavukcuoglu K, Kohli P, Hassabis D. Highly accurate protein structure prediction with AlphaFold. *Nature.* 2021;596:583–589.
20. Varadi M, Bertoni D, Magana P, Paramval U, Pidruchna I, Radhakrishnan M, Tsenkov M, Nair S, Mirdita M, Yeo J, Kovalevskiy O, Tunyasuvunakool K, Laydon A, Židek A, Tomlinson H, Hariharan D, Abrahamson J, Green T, Jumper J, Birney E, Steinegger M, Hassabis D, Velankar S. AlphaFold Protein Structure Database in 2024: providing structure coverage for over 214 million protein sequences. *Nucleic Acids Res.* 2024;52:D368-D375.
21. Evans R, O'Neill M, Pritzel A, Antropova N, Senior A, Green T, Židek A, Bates R, Blackwell S, Yim J, Ronneberger O, Bodenstein S, Zielinski M, Bridgland A, Potapenko A, Cowie A, Tunyasuvunakool K, Jain R, Clancy E, Kohli P, Jumper J, Hassabis D. Protein complex prediction with AlphaFold-Multimer. <https://www.biorxiv.org/content/10.1101/2021.10.04.463034v2#ref-2> (2021). [Last accessed 09/27/2024].
22. Abramson J, Adler J, Dunger J, Evans R, Green T, Pritzel A, Ronneberger O, Willmore L, Ballard AJ, Bambrick J, Bodenstein SW, Evans DA, Hung CC, O'Neill M, Reiman D, Tunyasuvunakool K, Wu Z, Žemgulytė A, Arvaniti E, Beattie C, Bertolli O, Bridgland A, Cherepanov A, Congreve M, Cowen-Rivers AI, Cowie A, Figurnov M, Fuchs FB, Gladman H, Jain R, Khan YA, Low CMR, Perlin K, Potapenko A, Savy P, Singh S, Stecula A, Thillaisundaram A, Tong C, Yakneen S, Zhong ED, Zielinski M, Židek A, Bapst V, Kohli P, Jaderberg M, Hassabis D, Jumper JM. Accurate structure prediction of biomolecular interactions with AlphaFold 3. *Nature.* 2024;630:493-500.

23. Meng EC, Goddard TD, Pettersen EF, Couch GS, Pearson ZJ, Morris JH, Ferrin TE. UCSF ChimeraX: Tools for structure building and analysis. *Protein Sci.* 2023;32:e4792.
24. Uniprot Consortium. UniProt: a worldwide hub of protein knowledge. *Nucleic Acids Res.* 2019;47:D506-515.
25. <https://www.ncbi.nlm.nih.gov/gene/2161#:~:text=Factor%20XII%20impairs%20arterial%20thrombus,but%20not%20in%20normal%20hemostasis>. [Last accessed 12/28/2023].
26. Litvak M, Shamanaev A, Zalawadiya S, Matafonov A, Kobrin A, Feener EP, Wallisch M, Tucker EI, McCarty OJT, Gailani D. Titanium is a potent inducer of contact activation: implications for intravascular devices. *J Thromb Haemost.* 2023;21:1200-1213.
27. Mohammed BM, Sun MF, Cheng Q, Litvak M, McCrae KR, Emsley J, McCarty OJT, Gailani D. High-molecular-weight kininogen interactions with the homologs prekallikrein and factor XI: importance to surface-induced coagulation. *J Thromb Haemost.* 2024;22:225-237.
28. Ivanov I, Verhamme IM, Sun MF, Mohammed B, Cheng Q, Matafonov A, Dickeson SK, Joseph K, Kaplan AP, Gailani D. Protease activity in single-chain prekallikrein. *Blood.* 2020;135:558-567.
29. Ivanov I, Matafonov A, Sun MF, Cheng Q, Dickeson SK, Verhamme IM, Emsley J, Gailani D. Proteolytic properties of single-chain factor XII: a mechanism for triggering contact activation. *Blood* 2017;129:1527-1537.
30. Frunt R, El Otmani H, Gibril Kaira B, de Maat S, Maas C. Factor XII Explored with AlphaFold – opportunities for selective drug development. *Thromb Haemost.* 2023;123:177-185.
31. Shamanaev A, Litvak M, Cheng Q, Ponczek M, Dickeson SK, Smith SA, Morrissey JH, Gailani D. A site on factor XII required for productive interactions with polyphosphate. *J Thromb Haemost.* 2023;21:1567-1579.
32. Ravon DM, Citarella F, Lubbers YT, Pascucci B, Hack CE. Monoclonal antibody F1 binds to the kringle domain of factor XII and induces enhanced susceptibility for cleavage by kallikrein. *Blood.* 1995;86:4134-4143.

33. Kohs TCL, Lorentz CU, Johnson J, Puy C, Olson SR, Shatzel JJ, Gailani D, Hinds MT, Tucker EI, Gruber A, McCarty OJT, Wallisch M. Development of Coagulation Factor XII Antibodies for Inhibiting Vascular Device-Related Thrombosis. *Cell Mol Bioeng.* 2020;14:161-175.
34. Iwaki T, Castellino FJ. Plasma levels of bradykinin are suppressed in factor XII-deficient mice. *Thromb Haemost.* 2006;95:1003–1010.
35. Revenko AS, Gao D, Crosby JR, Bhattacharjee G, Zhao C, May C, Gailani D, Monia BP, MacLeod AR. Selective depletion of plasma prekallikrein or coagulation factor XII inhibits thrombosis in mice without increased risk of bleeding. *Blood* 2011;118:5302-5311.
36. Pathak M, Kaira BG, Slater A, Emsley J. Cell Receptor and Cofactor Interactions of the Contact Activation System and Factor XI. *Front Med (Lausanne).* 2018;5:66.
37. Kaira BG, Slater A, McCrae KR, Dreveny I, Sumya U, Mutch NJ, Searle M, Emsley J. Factor XII and kininogen asymmetric assembly with gC1qR/C1QBP/P32 is governed by allostery. *Blood* 2020;136:1685-1697.
38. Emsley J, Saleem M, Li C, Phillipous H. Factor XII heavy chain structure [abstract]. Accessed September 30, 2023 at: [https:// abstracts.isth.org/factor-xii-heavy-chain-structure/](https://abstracts.isth.org/factor-xii-heavy-chain-structure/).
39. Law RH, Caradoc-Davies T, Cowieson N, Horvath AJ, Quek AJ, Encarnacao JA, Steer D, Cowan A, Zhang Q, Lu BG, Pike RN, Smith AI, Coughlin PB, Whisstock JC. The X-ray crystal structure of full-length human plasminogen. *Cell Rep.* 2012;1:185-190.
40. Chinnaraj M, Chen Z, Pelc LA, Grese Z, Bystranowska D, Di Cera E, Pozzi N. Structure of prothrombin in the closed form reveals new details on the mechanism of activation. *Sci Rep.* 2018;8:2945.
41. Mahdi F, Shariat-Madar Z, Todd RF 3rd, Figueroa CD, Schmaier AH. Expression and colocalization of cytokeratin 1 and urokinase plasminogen activator receptor on endothelial cells. *Blood* 2001;97:2342-2350.
42. Cheng Q, Tucker EI, Pine MS, Sisler I, Matafonov A, Sun MF, White-Adams TC, Smith SA, Hanson SR, McCarty OJ, Renné T, Gruber A, Gailani D. A role for factor XIIa-mediated factor XI activation in thrombus formation in vivo. *Blood* 2010;116:3981-3989.

43. Cool DE, Edgell CJ, Louie GV, Zoller MJ, Brayer GD, MacGillivray RT. Characterization of human blood coagulation factor XII cDNA. Prediction of the primary structure of factor XII and the tertiary structure of beta-factor XIIa. *J Biol Chem.* 1985;260:13666-71366.
44. Pozzi N, Bystranowska D, Zuo X, Di Cera E. Structural Architecture of Prothrombin in Solution Revealed by Single Molecule Spectroscopy. *J Biol Chem.* 2016;291:18107-18016.
45. Schrimpf W, Barth A, Hendrix J, Lamb DC. PAM: A Framework for Integrated Analysis of Imaging, Single-Molecule, and Ensemble Fluorescence Data. *Biophys J.* 2018;114:1518–1528.

**Table 1. Intramolecular Interactions (A) and Amino Acid Substitutions made in FXII (B).****A**

FN2 – CD	FN2 – KNG	KNG – Act loop	Act loop – CD
H35 → <u>G357</u>	<u>R36</u> → <u>L266</u>	T227 → <u>S349</u>	<u>R343</u> → Q482
H35 → <u>V359</u>	<u>R36</u> → <u>E225</u>	<u>D251</u> → <u>K346</u>	R345 → <u>E551</u>
<u>R36</u> → <u>E502</u>	Q33 → <u>S224</u>	<u>D253</u> → <u>K346</u>	<u>R353</u> → <u>G531</u>
<u>R36</u> → <u>V359</u>	L38 → D264	R265 → E411	<u>R353</u> → Q504
K45 → <u>Q501</u>	H40 → D264	<u>W268</u> → R362	
	<u>D61</u> → R229	<u>W257</u> => <u>K346</u>	
		<u>W268</u> => <u>K346</u>	

**B**

FN2	KNG	Act loop	CD
FXII-Arg36Ala	FXII-Glu225Ala	FXII-Arg343Ala	FXII-Val359Ala
FXII-Lys41Ala	FXII-Asn230Ala	FXII-Arg345Ala	FXII-Arg362Ala
FXII-Lys45Ala	FXII-Asp253Lys	FXII-Lys346Ala	FXII-Glu411Ala
FXII-Arg47Ala	FXII-Asp264Ala		FXII-Gln501Ala
	FXII-Arg265Ala		FXII-Glu502Ala
	FXII-Leu266Ala		FXII-Glu551Ala
	FXII-Trp268Ala		



## FIGURE LEGENDS

**Figure 1. A Model for human factor XII (FXII).** (A) Schematic diagram of human FXII showing the positions of the heavy chain N-terminal peptide (N-term, orange-red), fibronectin type 2 (FN2, purple), epidermal growth factor 1 (EGF1, brown), fibronectin type 1 (FN1, magenta), EGF2 (dark gray), and kringle (KNG, light green) domains, the proline-rich region (PRR, dark green), the activation loop (light gray) and the catalytic domain (CD, yellow). The position of an anion-binding site (ABS) between FN2 and EGF1 is indicated in light blue, the activation cleavage site at Arg<sup>353</sup> is indicated by a blue arrow, and the active site serine residue (Ser<sup>544</sup>) is indicated by the black bar. (B) AlphaFold adjusted prediction (Suppl. Fig. 3C) for full length human FXII shown as molecular surface representations. The two images shown are rotated 180° relative to each other. The color scheme is identical to that in panel A. Positions for the cleavage sites at Arg<sup>343</sup> and Arg<sup>353</sup> are indicated in dark blue. Most of the activation loop (Cys<sup>340</sup> to Arg<sup>353</sup>) is buried between the KNG and catalytic domains. (C) Predicted intramolecular interactions between the FXII FN2 domain (purple), KNG domain (light green), activation loop (light gray) and CD (yellow) are shown as cartoon and stick diagrams. Important basic amino acids are shown in dark blue, acidic amino acids in red and tryptophan residues in olive. Positions of Arg<sup>343</sup> and Arg<sup>353</sup> are indicated in dark blue on the peptide backbone of the activation loop. The side chain of Leu<sup>266</sup> is shown in light green and the position of Val<sup>359</sup> on the peptide backbone of the CD is indicated. Hydrogen bonds are shown as dashed light blue lines and cation- $\pi$  interactions as dashed orange lines.

**Figure 2. FXII activation.** (A-C). Activation of FXII by (A and B) PKa, or (C) FXIa. One hundred nanomolar wild type FXII (WT), FXII lacking most of its heavy chain region ( $\Delta$ FXII), or FXII variants with single amino acid substitutions were incubated with PKa (12.5nM) or FXIa (2.5 nM) at 37°C. For panels A through C, at indicated times aliquots were removed and tested for FXIIa generation by chromogenic assay. Results represent averages  $\pm$  one standard deviation for at least three experiments. (D) FXII cleavage by PKa. One micromolar FXII-WT (*left*) or the variant FXII-Ala<sup>346</sup> (*right*), was incubated with 125 nM PKa. At indicated time, samples were removed into reducing sample buffer and

size fractionated by SDS-PAGE. Positions of molecular mass standards are shown on the left. Shown on the right are positions of standards for the zymogen FXII band (Z) and the heavy chain (HC) and light chain (LC) of FXIIa. **(E)** Densitometric quantification of FXII zymogen band disappearance in reactions with PKa identical to those shown in Panel D. The curves show changes in zymogen band intensity as a percent of the intensity at 0 min. Each point represents the average for two experiments. **(F)** FXII-Ala544 (*left*), FXII-Ala268,Ala544 (*middle*) and FXII-Ala502,Ala544 (*right*), 100 nM each, was incubated with 12.5 nM PKa at 37°C. At indicated times, samples were removed into reducing SDS-sample buffer, size fractionated by SDS-PAGE and transferred to nitrocellulose membranes. Immunoblotting was with an HRP-conjugated anti-FXII IgG. Positions of molecular mass standards are shown on the left. Positions of standards for the zymogen (Z), and the heavy (HC), and light chains (LC) of FXIIa are indicated at the right of each image. Shown are representative blots for experiments that were run in duplicate.

**Figure 3. The FXII KNG Domain and Protein Conformation.** **(A)** FXII-WT (400 nM) was incubated with vehicle (*left panel*) or an equimolar concentration of IgG 5A12 (*right panel*). At indicated times samples were removed into reducing SDS-sample buffer, size fractionated by SDS-PAGE and transferred to nitrocellulose membranes. Immunoblotting was with an HRP-conjugated anti-FXII IgG. Positions of molecular mass standards are shown on the left. Positions of standards for the zymogen (Z), and the heavy (HC), and light chains (LC) of FXIIa are indicated at the right of each image. **(B)** FXII-WT, ΔFXII, FXII-Ala36, FXII-Lys253, and FXII-Ala346 (400 nM) were incubated overnight with an equimolar concentration of IgG 5A12. FXIIa generation was assessed by chromogenic substrate cleavage. **(C)** FXII-WT (WT), FXIIa-WT (XIIa), FXII-Lys253, and FXII-Ala346 (200ng) were size fractionated by SDS-PAGE, transferred to nitrocellulose membrane, and immunoblotted with IgG 5A12 (*left and middle*) or polyclonal anti-FXII IgG (*right*). **(D)** One hundred nanomolar FXII-WT (WT), ΔFXII or FXII-WT mixed with 100nM IgG 5A12 (WT + 5A12) was incubated with PKa (12.5nM) at 37°C. At indicated times aliquots were removed and tested for FXIIa generation by chromogenic assay. **(E)** smFRET efficiency histograms of FXII S544A in the absence (*left panel*) or presence (*right panel*) of 100mM εACA. Representative graphs are shown. Each experiment was done in triplicate. Gaussian distribution is indicated by red dashed lines. The number of each population is indicated at the left of each image.

**Figure 4. FXII binding to PK.** (A) Standard curve of different concentrations (1-120  $\mu\text{g/ml}$ ) of wild type FXII or FXIIa binding to plate-immobilized PK. Results are shown as OD values, measured as described in the Methods Section. (B) Binding of wild type FXII and FXIIa, and FXII variants (30  $\mu\text{g/ml}$ ) to plate-immobilized PK. Values are shown as a percent of the signal for FXII-WT (assigned a value of 100%)  $\pm$  one SD. (C) Plasma FXII or FXIIa (10  $\mu\text{g}$ ) were incubated overnight with anti-PK IgG-beads alone or with plasma PK (10 $\mu\text{g}$ ) at 4°C. (D) Plasma or recombinant FXII (10 $\mu\text{g}$ ) were incubated overnight with anti-PK IgG-beads and 10 $\mu\text{g}$  PK lacking an active site serine (PK-Ala559) at 4°C. For panels C and D. After incubation, the beads were washed, samples were eluted with non-reducing SDS-sample buffer, size fractionated by SDS-PAGE, and either (C) stained with Coomassie blue or (D) transferred to nitrocellulose membranes and probed with anti-FXII HRP-conjugated IgG. Positions of molecular mass standards are shown on the left. Positions of standards for PK and FXII/FXIIa are indicated at the right of each image. Shown are representative gels/blots for experiments that were run in duplicate.

**Figure 5. Activation of the Kallikrein-Kinin System in human plasma.** (A) Human FXII-deficient plasma was supplemented with 400 nM FXII-WT and incubated in the presence (*top row*) or absence (*bottom row*) of kaolin (2.5 mg/ml). Kaolin will induce contact activation in plasma. (B) Human FXII-deficient plasma was supplemented with 400 nM FXII-Ala<sup>36</sup> (*top row*) or FXII-Ala<sup>346</sup> (*bottom row*). For all experiments, FXII supplemented plasma was incubated at 37°C. Samples were removed at the indicated times into non-reducing sample buffer, size fractionated by SDS-PAGE and transferred to nitrocellulose membranes. Membranes were developed with antibodies to FXII (*left*), PK (*middle*) or FXI (*right*). Positions of molecular mass standards in kilodaltons are shown to the left of each panel. Positions for free FXII and FXIIa (XII(a)), free PK and PKa (PK(a)) and FXI and FXIa; and FXIIa, PKa and FXIa in complex with plasma protease inhibitors (XIIa + INH, PKa + INH and XIa + INH) are shown to the right of each panel. Note that free FXIa migrates more slowly than free FXI (A, *right column*). Shown are representative blots for experiments that were run in duplicate.

**Figure 6. HK cleavage in human plasma and in mice.** (A) Human FXII-deficient plasma was supplemented with FXII-WT,  $\Delta$ FXII, FXII-Ala<sup>36</sup>, FXII-Lys<sup>253</sup> and FXII-Ala<sup>346</sup> (140 nM) and incubated

at 37°C. At indicated times, samples were removed into non-reducing sample buffer, transferred to nitrocellulose membranes and probed with goat anti-human HK IgG. Positions of markers for uncleaved HK (white arrow) and cleaved HKa forms (black arrows) are indicated to the right of each image. Western blots underwent densitometry scanning to generate the curves shown below each western blot. Curves show the disappearance of HK (blue), appearance of HKa intermediate (single cleavage, gray), and appearance of the final form of HKa (two cleavages, red). Percentile values were assigned to each band based on comparison to the density of the HK band at time zero (assigned a value of 100%). Data are averages of 2 experiments. **(B)** FXII deficient mice received intravenous infusions of FXII-WT,  $\Delta$ FXII, FXII-Ala36, FXII-Lys253 or FXII-Ala346 to achieve estimated plasma concentrations of 40nM. Shown are nonreducing western blots of plasma collected 0, 15, or 30 minutes, or ~16 hours (O/N, overnight) after infusion. Blots were developed with anti-murine HK IgG. Positions of markers for HK (white arrows) and cleaved HKa forms (black arrows) are indicated to the right of each image. Positions of molecular mass markers are shown on the left. Shown are representative blots for experiments that were run in duplicate.

Figure 1

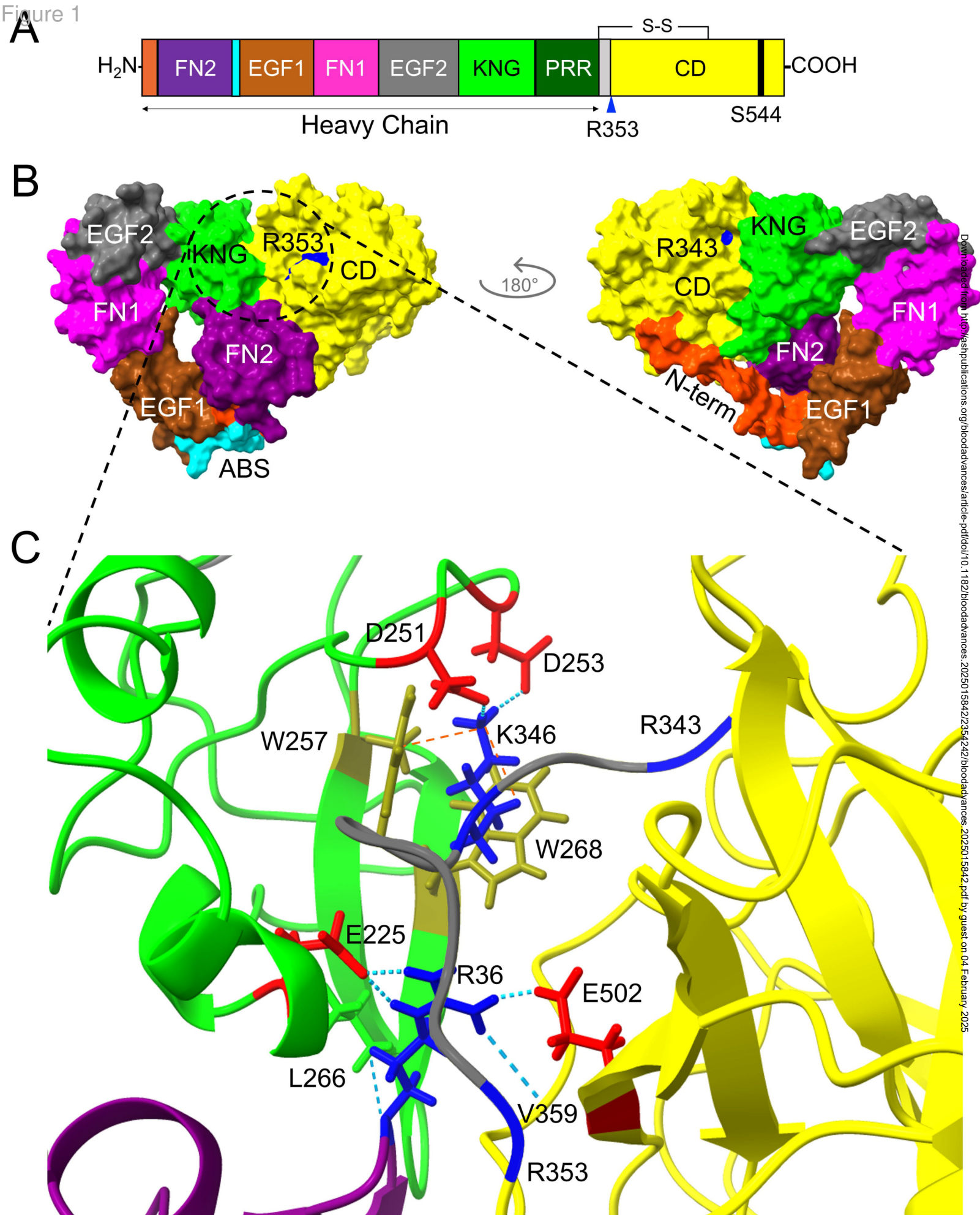


Figure 1

Figure 2

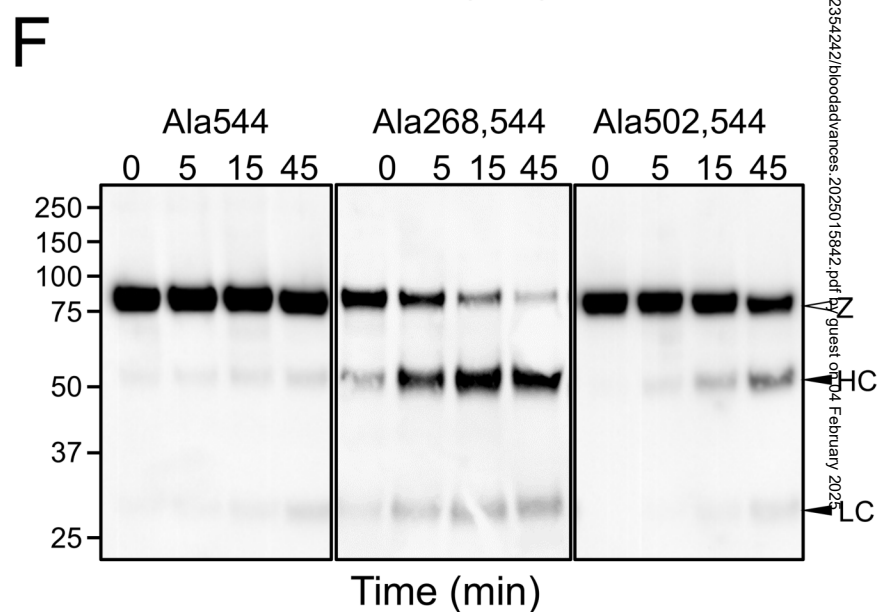
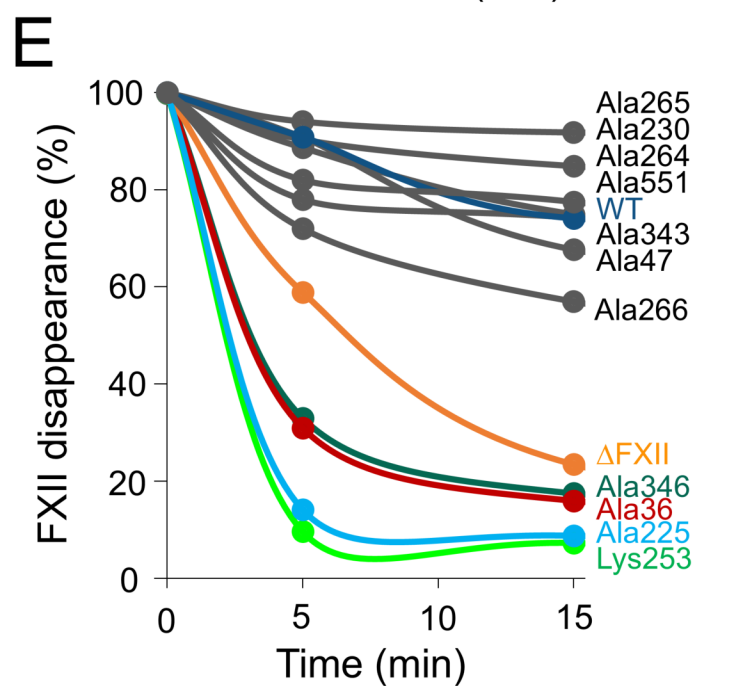
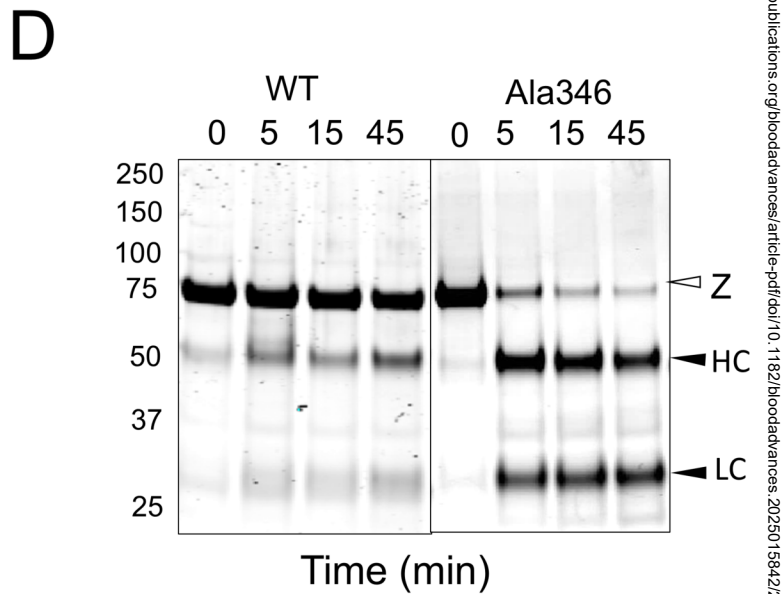
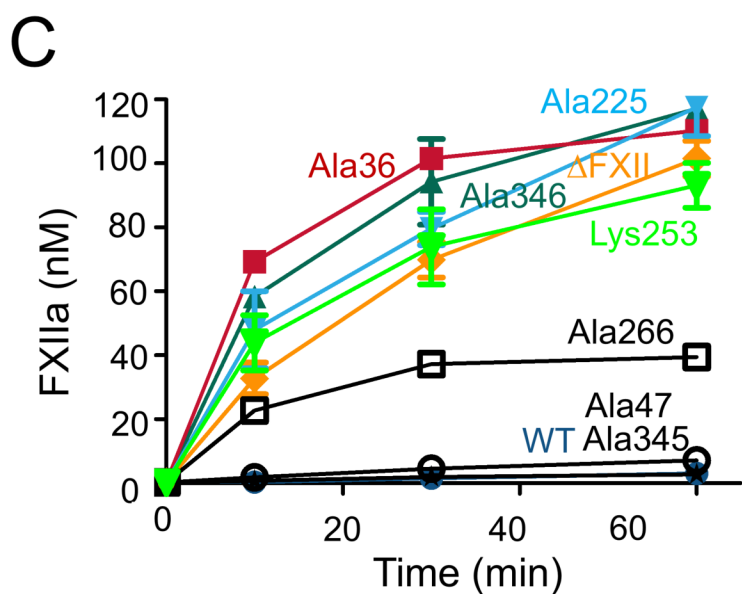
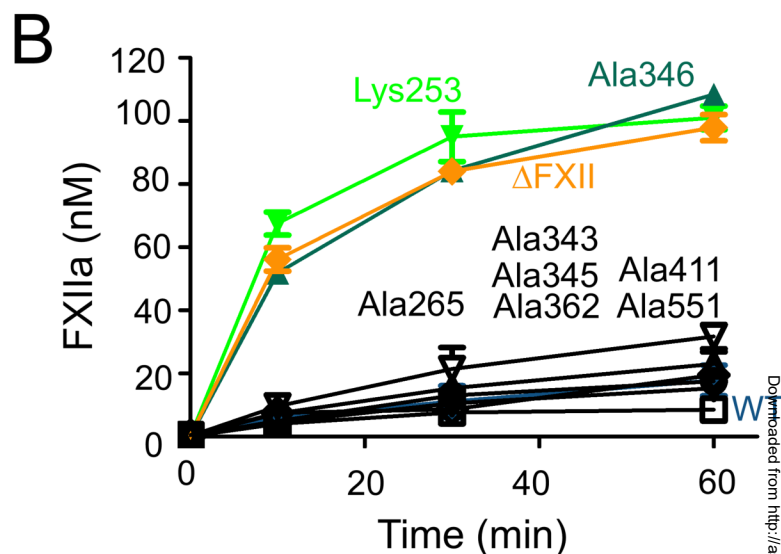
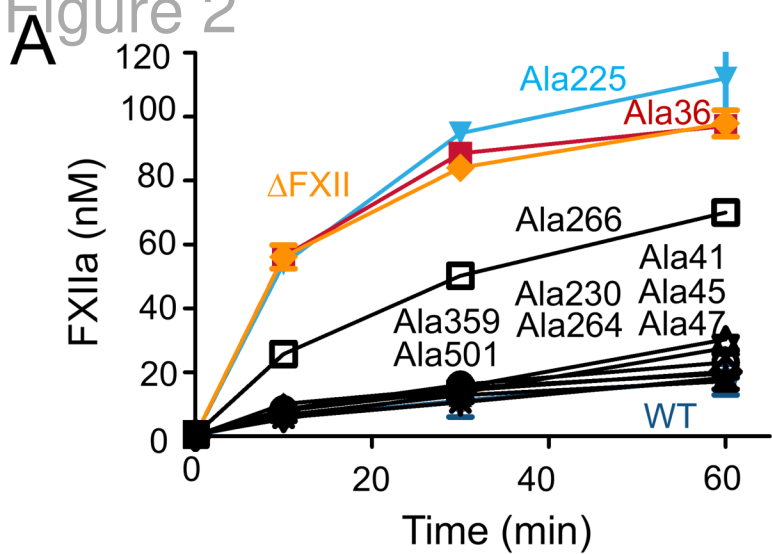


Figure 2

Figure 3

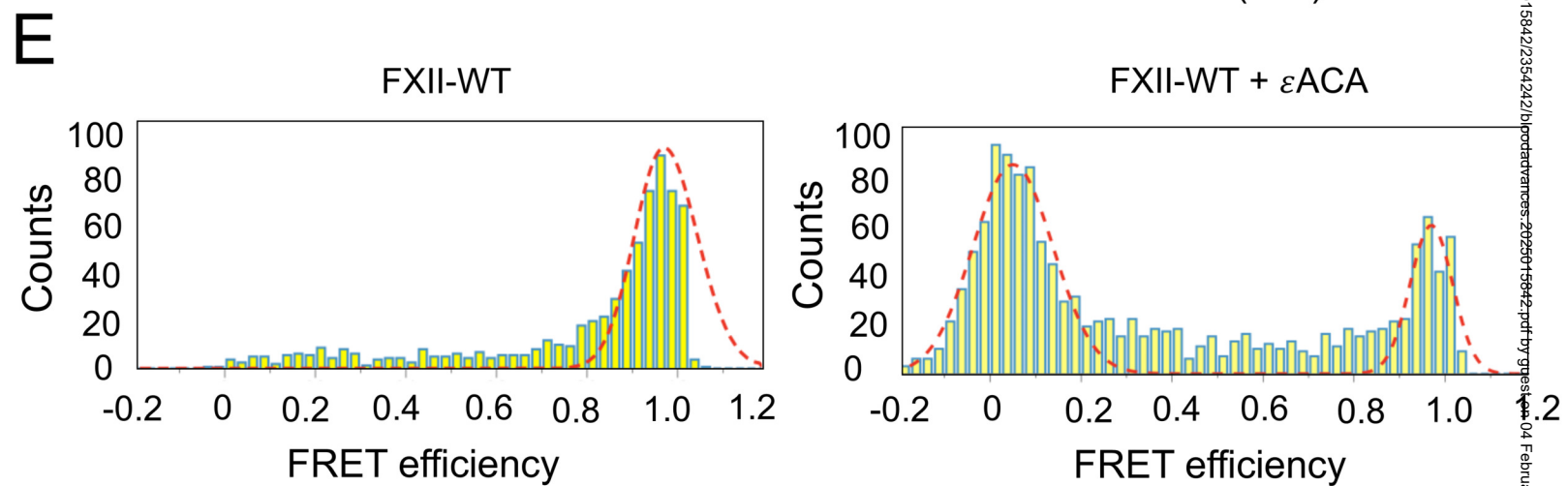
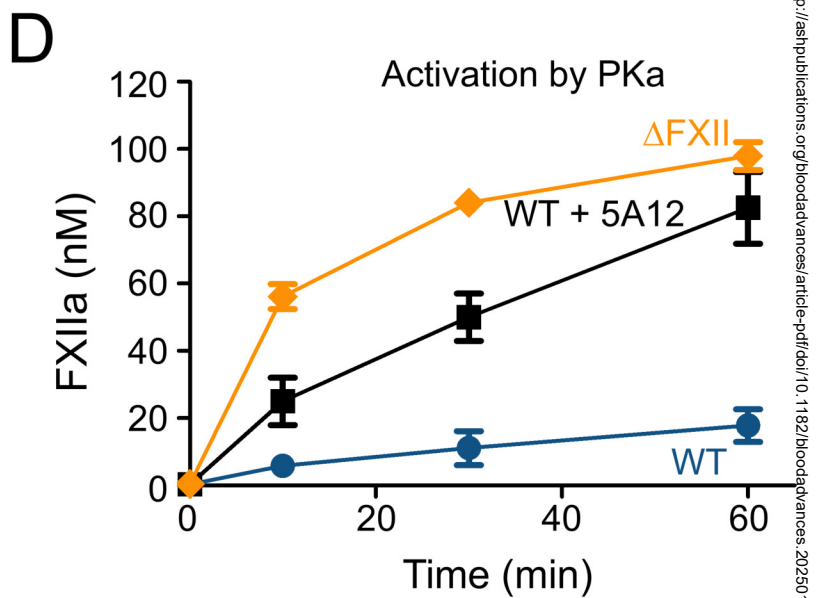
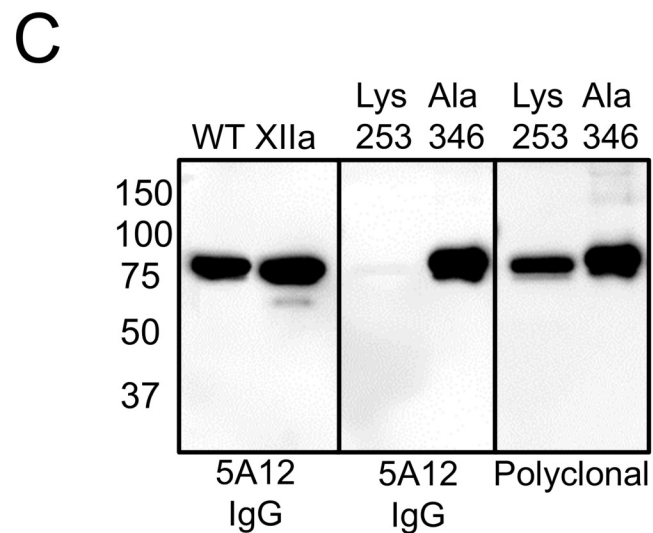
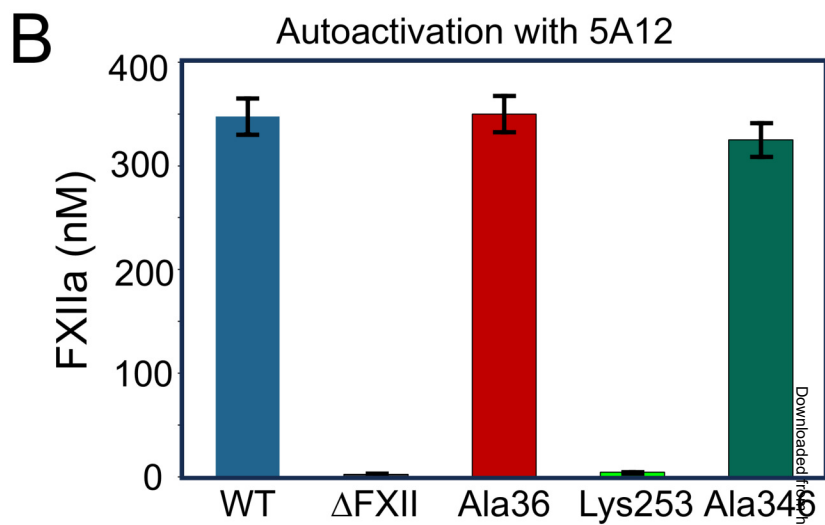
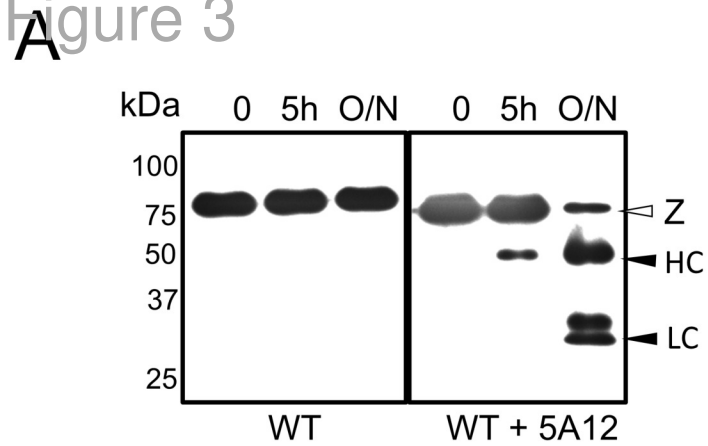
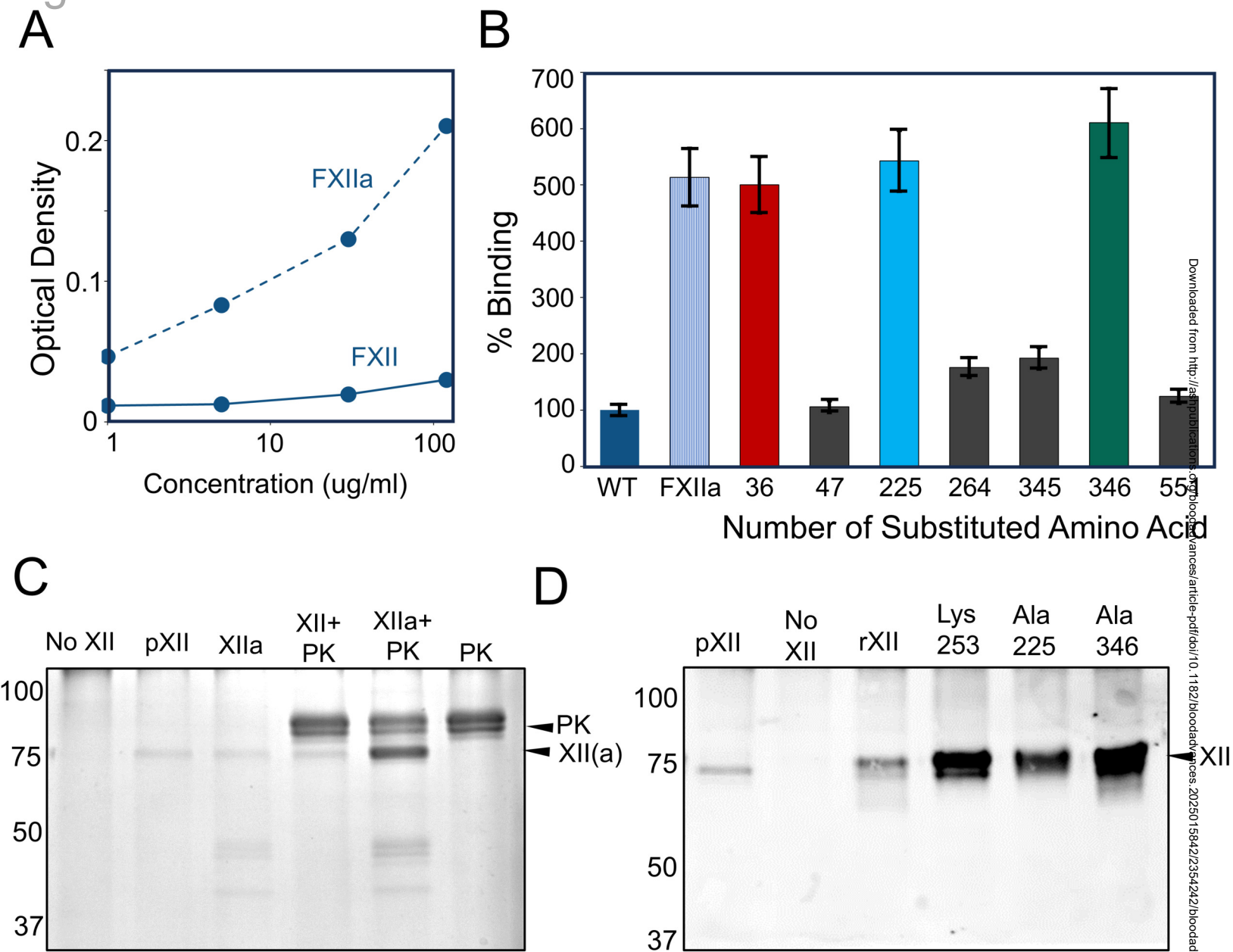


Figure 3

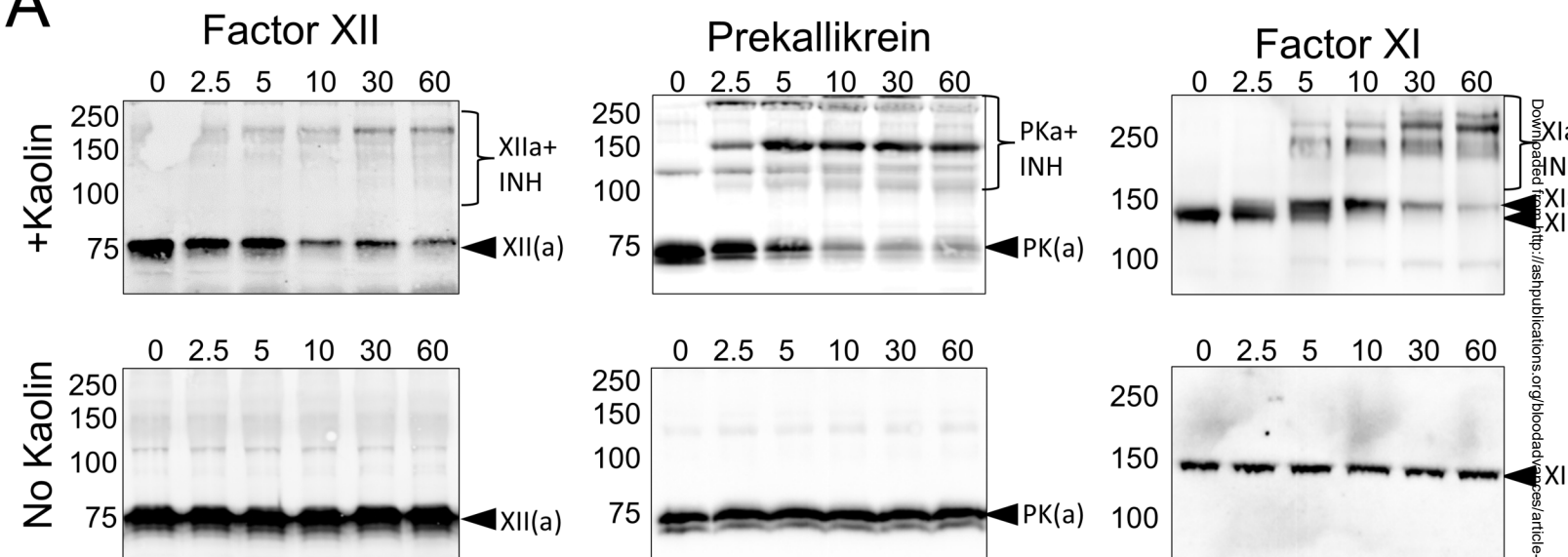
Figure 4



Downloaded from <http://aspubs.oxfordjournals.org/advance-article-pdf/doi/10.1182/bloodadvances.2025015842/2354242/bloodadvances.2025015842.pdf> by guest on 04 February 2025

Figure 4

**A**



**B**

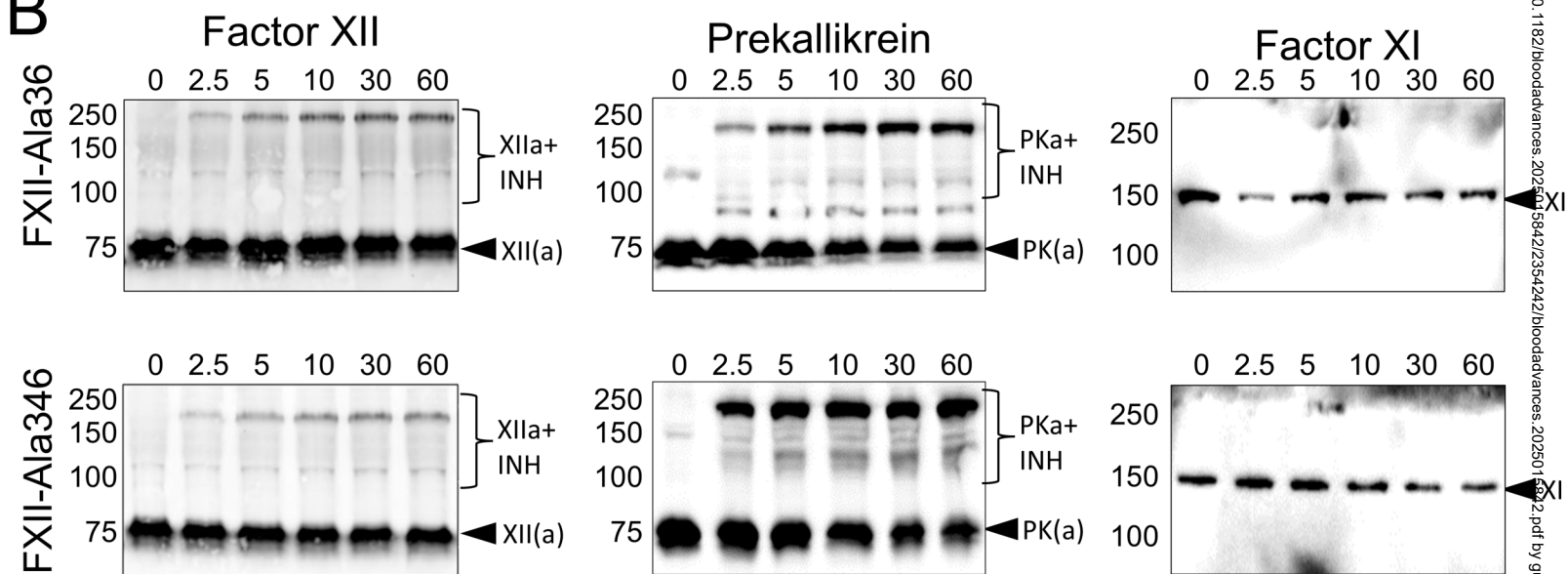
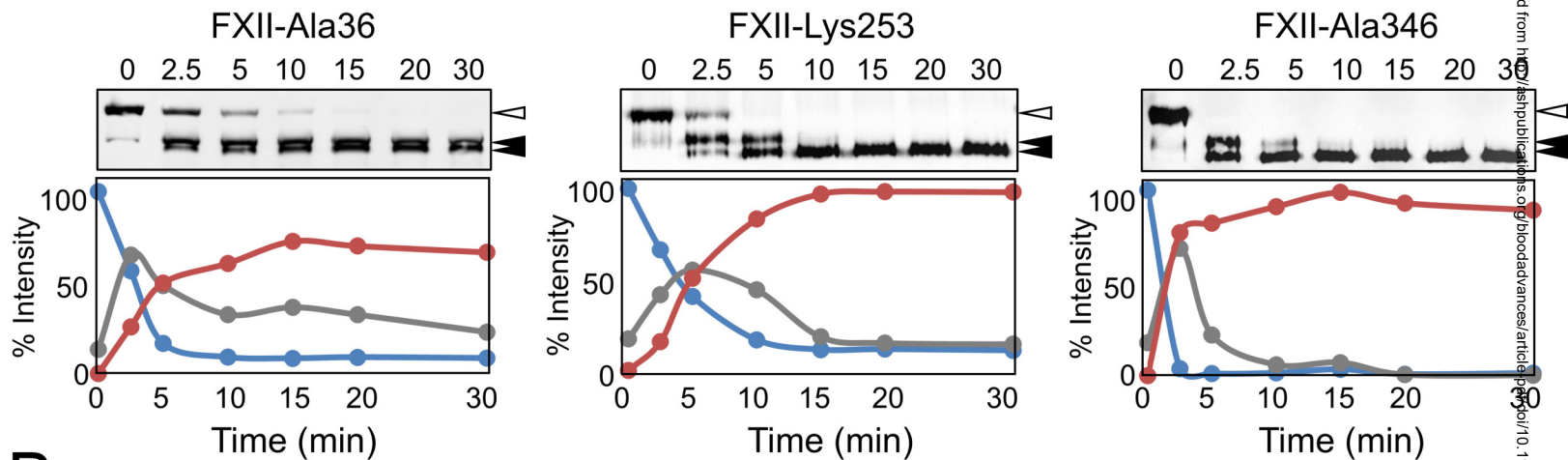
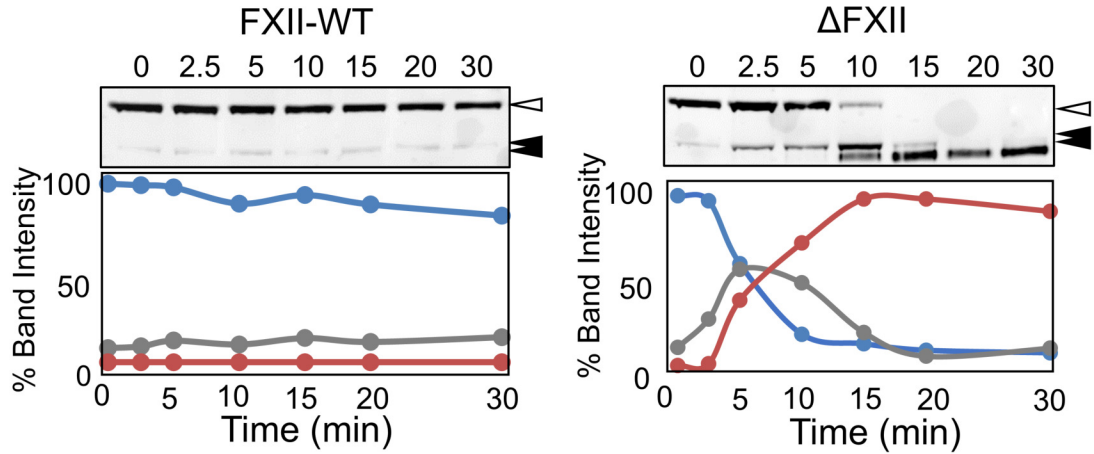
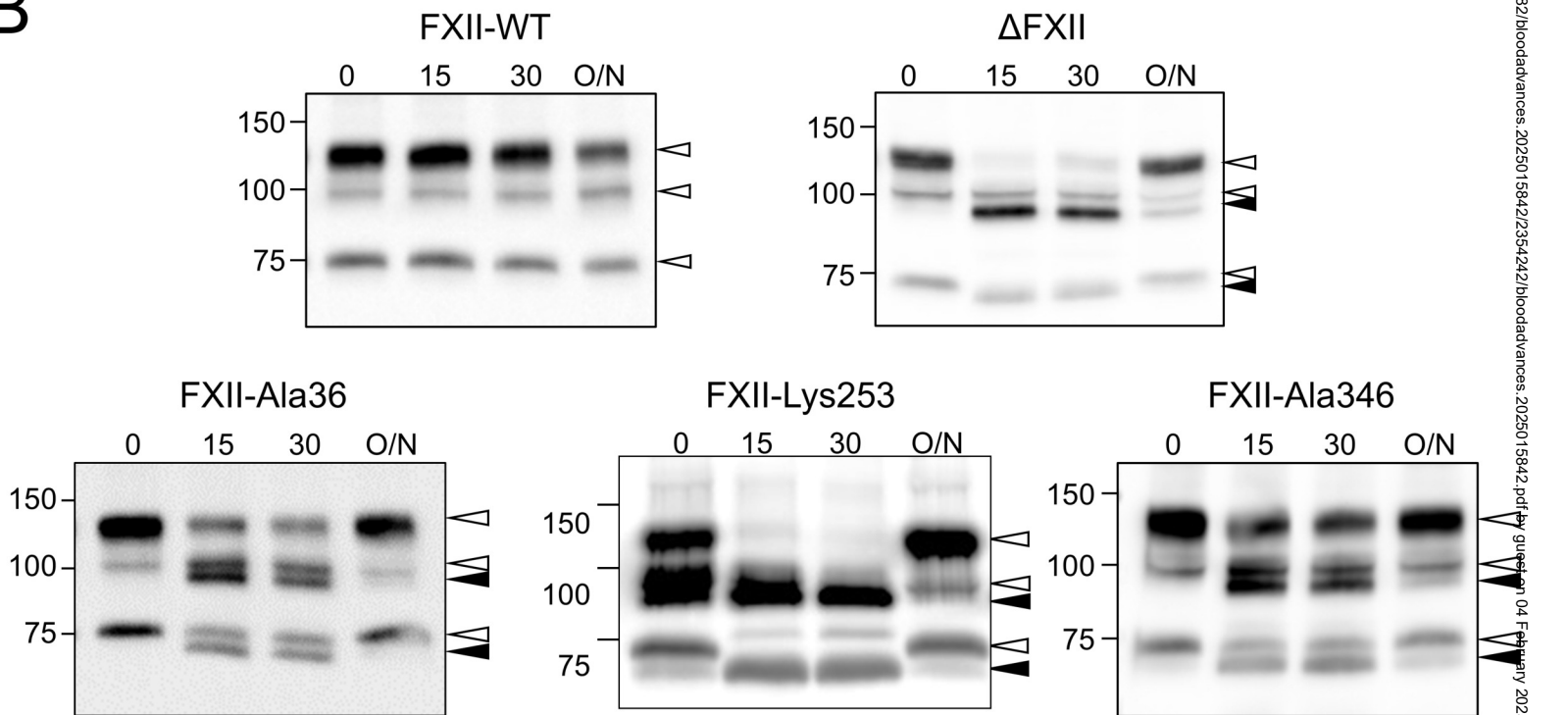


Figure 6

A



B



Downloaded from https://pubs.aip.org/journal-of-biochemical-advances/article-pdf/doi/10.1182/jbioadvances.2025015842/2354242/jbioadvances.2025015842.pdf by guest on 04 February 2025

Figure 6